IEICE TRANS. ELECTRON., VOL.E93–C, NO.11 NOVEMBER 2010

INVITED PAPER *Special Section on Electronic Displays*

A Quantitative Evaluation Method for Luminance Non-uniformity of a Large LED Backlight

Yuko MASAKURA[†a)], **Tohru TAMURA**[†], **Kunihiko NAGAMINE**[††], **Satoshi TOMIOKA**[††], **Mitsunori UEDA**[††], *and* **Yoshihide SHIMPUKU**[††], *Nonmembers*

SUMMARY This report describes a quantification method for luminance non-uniformity of a large LED backlight. In experiments described herein, participants subjectively evaluated artificial indistinct Mura images that simulated luminance non-uniformity of an LED backlight. We measured the luminance distribution of the Mura images. Then, the measured luminance distribution was converted into S-CIELAB, in which anisotropic properties of the spatial frequency response of human vision were considered. Subsequently, some indexes for the quantification model were extracted. We conducted multiple regression analyses using the subjective evaluation value and the index values obtained from measured luminance of Mura image. We proposed a quantification model consisting of four indexes: high and low luminance area, number of Mura edges, sum of Mura edge areas, and maximum luminance difference.

key words: *luminance non-uniformity, LED backlight, subjective evaluation, quantification method*

1. Introduction

With digital TV broadcasting in recent years, large flat panel displays, for example liquid crystal displays (LCDs) and plasma display panels (PDPs), have grown popular as displays for high-quality images. It is therefore increasingly important to improve the image quality of flat panel displays. One factor degrading the image quality is luminance non-uniformity: so-called Mura. The Mura of an LCD is classified into two types [1]. One is called cluster Mura which is visible as a small dark spot or a thin line caused by cracks in the color filter, contamination in the cell, and so on. Another is called indistinct Mura which shows luminance gradients caused by non-uniformity of the backlight or the cell. These are the important factors affecting image quality not only in LCDs but also in other displays.

Light emitting diodes (LEDs) are used as light sources of cellular phones, signal lights, game devices, and so on. There are also used as a new backlight source of LCDs: recently LCDs with LED backlighting have been manufactured. Cold cathode fluorescent lamps (CCFLs) have been mainly used as backlight sources of LCDs. Although LEDs are more expensive than CCFLs, they present many advantages such as high-fidelity color reproduction and long life. Considering the luminance uniformity of the LED backlight, a dark area is generated easily because LEDs are point light sources [2]. For a large LED backlight, many dark areas would generate indistinct Mura phenomena.

The predominant evaluation method for Mura inspection is visual analysis conducted by experienced inspectors. Although visual inspection by the inspectors is an excellent method and generates good results, it usually requires a long time and many people; it typically incurs high costs. Therefore, the need exists to inspect Mura using optically measured criteria that correspond with human perception. Previous reports [3]–[8] have described studies of quantitative evaluation methods for cluster Mura of LCDs based on sensory analyses. A formula was proposed to estimate the just noticeable difference (JND) contrast on various background luminance levels using cluster Mura which formed rectangles, circles, and lines with various sizes [8]. In other early reports [9], [10], a method for Mura inspection by a spatial standard observer (SSO) was proposed. The SSO is a model of human sensitivity to spatial contrast patterns. This model is expected to be useful for detecting major defects in a display.

On the other hand, previous reports [11], [12] have explained quantitative evaluation methods for indistinct Mura. In a previous study by the authors [12], the luminance non-uniformity of a basic module which consists of four LEDs were simulated by changing each LED brightness and artificial indistinct Mura images with five forms which showed dark polarity against a rectangular background with 11 inches diagonal were evaluated subjectively. Results showed that three numerical indexes based on measured luminance of Mura image — "low luminance area against background," "Mura edge area" and "maximum of luminance difference between Mura and the uniform image" — were significant for predicting the subjective evaluation value of indistinct Mura. In actual, however, an LED backlight has many basic modules in array. So it would not be enough to consider the way to quantify subjective evaluation for Mura of an actual LED backlight.

In this report, we present results of experiments that were conducted to evaluate artificial Mura images with more complex forms, larger size, and both dark and bright polarities presented on a 40-inch LCD TV display. Mura images presented for subjective evaluation were assumed as a 40-inch LED backlight composed of LED modules placed on a matrix of 28×16. We propose a quantitative evaluation method for luminance non-uniformity of a large LED backlight using indexes based on the measured luminance of a

Manuscript received March 1, 2010.
Manuscript revised June 10, 2010.

[†]The authors are with Tokyo Polytechnic University, Atsugi-shi, 243-0297 Japan.
[††]The authors are with SONY Co., Tokyo, 108-0075 Japan.
a) E-mail: masakura@mega.t-kougei.ac.jp

DOI: 10.1587/transele.E93.C.1564

Mura image.

2. Experiment 1

2.1 Methods

2.1.1 Stimuli and Apparatus

Luminance non-uniformity images, so-called Mura images, used in the experiment were made using the following procedures. We produced the Mura images based on a design of an actual LED backlight, and so Mura phenomena of an LED backlight could be simulated as faithfully as possible. The luminance profiles of an LED module at various brightness levels were measured using a two-dimensional luminance meter. A uniform part was subtracted from the luminance profile and the fundamental form of non-uniformity image was made. This fundamental form will be called the Mura element hereinafter. In this study, the Mura element had a similar shape to that of a Gaussian because it used an LED with the radiation angle distribution of a Lambertian. The Mura elements of six kinds of contrast of both bright and dark polarities (±15, ±9, ±6, ±3, ±2, and ±1%, presented in Fig. 1) were made by expanding or reducing the Mura element without changing the fundamental form. The definition of the contrast was a peak luminance difference from the background (154 cd/m^2). In the experiments, a 40-inch backlight was assumed whose LED module was placed on a 28 × 16 matrix (31.8 mm pitch) unit. Mura elements were arranged simulating that backlight (see the upper panel in Fig. 2). The adjoined Mura elements were mutually overlapped because the full width at half maximum of a Mura element was 47.2 mm. This overlapped part was assumed to be additive processing considering actual ray multiplication. Details of the method of producing the Mura image are presented below.

The 28 × 16 matrix was divided into eight areas. Each area had 7 × 8 units. Contrast ranges of three kinds (±15, ±9, ±6%) and arrangement densities of two kinds (30, 90%) were combined for the experimental conditions. The arrangement density means the ratio of number of the Mura elements that were arranged in a pattern to 56 (7 × 8). The values of these two parameters, the contrast range and the arrangement density, were chosen so that Mura was not too worse and not too difficult to recognize based on authors' visual judgments under the same environment as that in the experiment. Five luminance non-uniformity patterns (Mura pattern P1-P5) were prepared (Table 1). In the case of Mura pattern 3 (P3), for example, Mura elements with −9 to +9% contrast were arranged at the arrangement density 30%, that is, at 16 places (50 places in case of 90%) that had been chosen at random among 56 places (Fig. 2). By combining three Mura patterns (repetition was included) of the choice from these five Mura patterns, evaluation stimuli of 35 kinds were produced (Table 2). The Mura elements were arranged

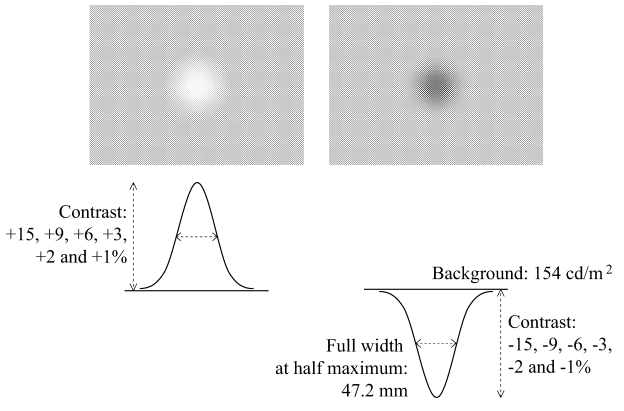

Fig. 1 Luminance characteristics in Mura element.

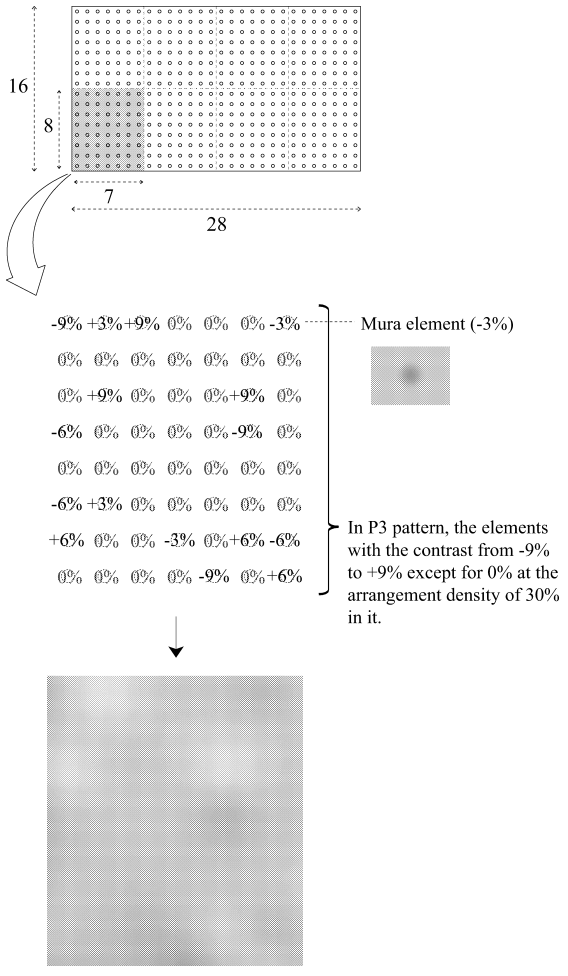

Fig. 2 Mura elements arrangement to make a Mura pattern (e.g., P3).

Table 1 Contrast range and arrangement density in each Mura pattern.

	Contrast range	Arrangement density
P1	±15%	30%
P2		90%
P3	±9%	30%
P4		90%
P5	±6%	90%

Table 2 Mura pattern combinations and conditions in each evaluation stimulus. Condition in bold character represents one used for Experiment 2.

P1-P1-P1	**P1-P1-P2**	**P1-P1-P3**	P1-P1-P4	P1-P1-P5	P1-P2-P2
P1-P2-P3	**P1-P2-P4**	P1-P2-P5	P1-P3-P3	P1-P3-P4	**P1-P3-P5**
P1-P4-P4	P1-P4-P5	**P1-P5-P5**	**P2-P2-P2**	P2-P2-P3	**P2-P2-P4**
P2-P2-P5	**P2-P3-P3**	**P2-P3-P4**	**P2-P3-P5**	**P2-P4-P4**	P2-P4-P5
P2-P5-P5	**P3-P3-P3**	P3-P3-P4	P3-P3-P5	P3-P4-P4	**P3-P4-P5**
P3-P5-P5	P4-P4-P4	P4-P4-P5	**P4-P5-P5**	P5-P5-P5	
±1% (contrast range), 30% (arrangement density)				**±1%, 90%**	
±2%, 30%	**±2%, 90%**	±3%, 30%	±3%, 90%	**Uniform image**	

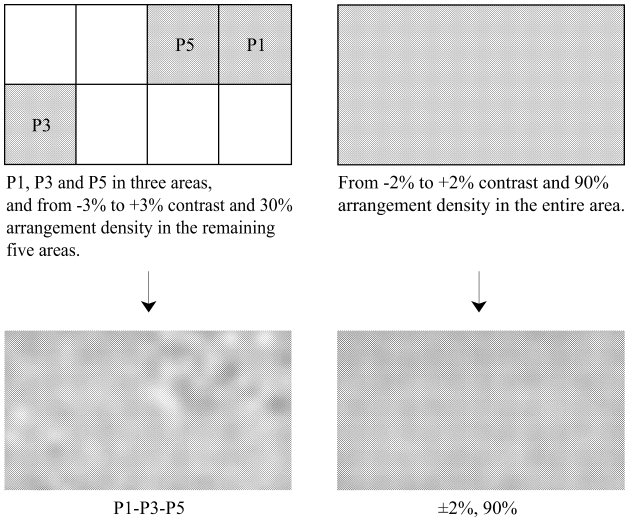

Fig. 3 Sample of evaluation stimulus.

at random in every combination. Therefore, the order of row of the Mura element was different in each Mura pattern, although the contrast range and the arrangement density used to produce a Mura pattern were kept constant.

Each combination of Mura pattern in Table 2 was arranged in three areas that were selected randomly from eight areas. The Mura image was made by arranging Mura patterns with ±3% contrast range and 30% arrangement density in the remaining five areas (e.g., left of Fig. 3). Aside from these 35 Mura images, six Mura images (Table 2) in which the Mura elements with a contrast range of three kinds (±1, ±2, ±3%) and an arrangement density of two kinds (30, 90%) were arranged in all the areas were prepared (e.g., right of Fig. 3). A uniform luminance image was also made; these 42 images were used as evaluation stimuli in the experiment (Table 2). In the subjective evaluation, one Mura image (standard stimulus) was prepared aside from the evaluation stimuli. A standard stimulus was assumed for which the level of luminance non-uniformity was slightly lower than the average level of evaluation stimuli so that the participants could evaluate them easily.

Two signal generators (VG-870, VG-849; ASTRO) and two 40-inch liquid crystal displays (BRAVIA KDL-X2500, SONY, 1920 × 1080 pixel resolution) were used for presenting the Mura images. The display was remodeled to reduce its own luminance non-uniformity by increasing the distance

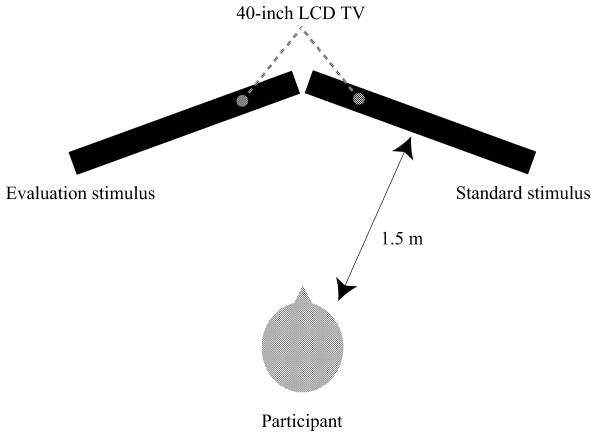

Fig. 4 Experimental environment.

between light source and a diffuser plate. And the result of 448 points measurement data in the whole screen showed, the average brightness was 163 cd/m^2 and the maximum brightness was 174 cd/m^2. Two displays were arranged side by side in front of a participant, the evaluation stimulus was presented on the left side one; the standard stimulus was presented on the right side one (Fig. 4). The experiment was conducted in a darkroom, and a distance from the participant to the display was 1.5 m.

2.1.2 Procedures

The ITU-R five-grade impairment scale [13] is well known as a method for subjective assessment of image quality. However, it is necessary to obtain a subjective evaluation value of Mura as a continuous and proportional scale to show a continuous relation between characteristics of Mura image and subjective evaluation value. In the experiment, therefore, the evaluation stimuli were evaluated using the magnitude estimation (ME) method [14]. In the experiment, participants answered a numerical value, we called it an ME value, that corresponded to the grade of non-uniformity of the evaluation stimulus comparing with the grade of the standard stimulus as 100. A higher ME value means that the evaluation of Mura is worse. In all, 42 evaluation stimuli were evaluated by repeating this procedure.

2.1.3 Participants

In the experiment, 31 participants (19 male and 12 female; 21–23 years old), took part. Each had visual acuity higher than 0.7.

2.2 Index Extraction

2.2.1 Conversion of Measurements Based on Human Vision

Luminance distributions of the 42 Mura images were measured using a two-dimensional luminance colorimeter

(ICAM-3FW, DELTA, 1280 × 960 pixel resolution). They were subsequently converted to L^* images (16 bit, 1234 × 689 pixel) using the extended S-CIELAB model [15].

In fact, S-CIELAB is a spatial extension of the CIELAB color metric. It is useful for measuring color reproduction errors of digital images [16]. In calculating S-CIELAB, the image data are transformed into opponent-color spaces. Each opponent-color image is convolved with the visual spatial sensitivity filter to that color dimension; then the filtered images are transformed to CIELAB. Two dimensional isotropic filters are used in S-CIELAB. However the spatial frequency response of human vision has dependence of directivity [17]. The extended S-CIELAB [15] in which this anisotropic property of the spatial frequency response of human vision is considered can measure color reproduction errors of digital images more suitable for human vision.

In this study, we examine the predicting model for ME value using L^* as calculated using the extended S-CIELAB model.

2.2.2 Luminance Distribution Characteristics of Mura

The nine indexes of characteristics of Mura image (Table 3) were calculated to examine the relation to the ME value as explained below.

Table 3 Indexes as explanatory variables used in the analyses.

(a)	High and low luminance area ($\Delta L^* \geqq 1$)
(b)	($\Delta L^* \geqq 2$)
(c)	($\Delta L^* \geqq 3$)
(d)	($\Delta L^* \geqq 4$)
(e)	Number of Mura edges
(f)	Sum of Mura edge areas
(g)	Sum of Mura edge lengths
(h)	Average of Mura edge circularities
(i)	Maximum luminance difference

The mean value of L^* of all pixels in the L^* image was subtracted from L^* of each pixel; it was assumed that ΔL^*. Then the ratio to all pixel counts (1234×689) of pixel counts was calculated where this difference was larger than the constant value from 1 to 4. These ratios were defined as four of the nine indexes: those were (a–d) high and low luminance areas (a: $\Delta L^* \geqq 1$, b: $\Delta L^* \geqq 2$, c: $\Delta L^* \geqq 3$, d: $\Delta L^* \geqq 4$). These indexes correspond to the area for which participants would recognize a brighter or darker area of the Mura image.

A 3 × 3 Sobel filter was processed to extract the area within which luminance changed gradually, and where edge pixels of one pixel were filtered out as noise. The remaining edge areas were labeled. This label number was defined as (e) number of Mura edges. The ratio to all pixel counts of the detected edge pixel count was defined as (f) sum of Mura edge areas. Furthermore, the ratio to all pixel counts of the detected edge pixel count in surroundings of each label was defined as (g) sum of Mura edge lengths. The circularity of each label was calculated using the following expression: $(\text{edge length})^2/(4\pi \times \text{edge area})$, and averaged by label number. This value was defined as (h) average of Mura edge circularities. Indexes (e) and (f) would correspond to the area with luminance change in Mura images, and indexes (g) and (h) correspond to the shape complexity of this area. The Sobel filter threshold was selected so that the correlations between indexes were low, although the correlations between each index of edge and ME value were high. The threshold corresponds to $\Delta L^* = 2$/mm on the display.

The maximum difference from average L^* of L^* image was defined as (i) maximum luminance difference. This index corresponds to the Mura contrast. These nine indexes (Table 3) were used as explanatory variables in analyses.

2.3 Analyses for the Predicting Model

The ME values were standardized so that each participant's

Table 4 Results for the multiple regression analyses.

		Partial regression coefficient B	Standard error of B	Standardized partial regression coefficient β	t	Adjusted R^2	F	Variance inflation factor
Model A	Constant	-2.52	0.14		-17.44 *	0.96	300.92 *	
	Index (e)	0.0025	2.63E-04	0.32	9.40 *			1.08
	(f)	8.27	1.08	0.51	7.66 *			4.25
	(i)	0.080	0.01	0.36	5.35 *			4.21
Model B	Constant	-2.27	0.17		-13.30 *	0.92	182.52 *	
	Index (e)	0.0015	2.10E-04	0.31	7.41 *			1.06
	(f)	11.28	0.90	0.73	12.52 *			1.99
	(i)	0.066	0.01	0.30	4.98 *			2.08
Model C	Constant	-2.80	0.29		-9.54 *	0.93	149.90 *	
	Index (a)	1.58	0.73	0.18	2.15 *			4.51
	(e)	8.77E-04	3.60E-04	0.18	2.43 *			3.54
	(f)	10.13	1.01	0.65	9.99 *			2.74
	(i)	0.056	0.01	0.25	4.12 *			2.37

* $p < .01$

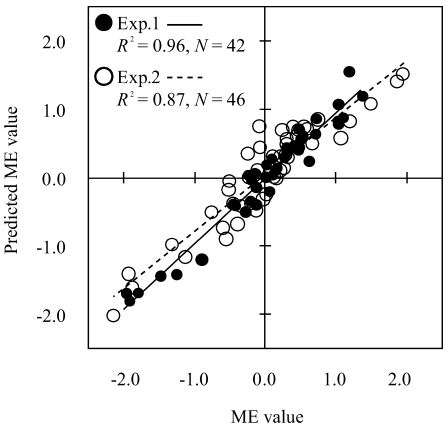

Fig. 5 Relation between the ME value and the predicted ME value calculated from Model A.

average of all conditions equals to 0 and the standard deviation equals to 1 because the raw ME values have different ranges and variations among participants. To extract effective indexes for predicting the ME value, we first conducted a multiple regression analysis (with forced entry of all variables) with the ME value as a dependent variable and the value of nine indexes [(a–i)] as explanatory variables. Results of the analysis show that three indexes, which were (e) number of Mura edges [t (32) = 2.55, $p < .05$], (f) sum of Mura edge areas [t (32) = 3.42, $p < .01$], and (i) maximum luminance difference [t (32) = 4.75, $p < .001$] would be significant for predicting the ME value. For the subsequent analysis, we conducted another multiple regression analysis (with forced entry of all variables) with the ME value as a dependent variable and the values of these three indexes as explanatory variables (Model A, Table 4). In this model, variance inflation factors (VIFs) that indicate the multicolinearity between explanatory variables were less than 10, suggesting the significances and reliabilities of the explanatory variables. The ME value (Y) was calculated using the following equation.

$$Y = 0.0025X_e + 8.27X_f + 0.080X_i - 2.52 \quad \text{(A)}$$

Y: ME value, X_a–X_i: value of respective indexes

2.4 Discussion

Figure 5 (•) shows the relation between the ME value and the predicted ME value from Model A. The value of the coefficient of determination (R^2) between the ME value and the predicted ME value was 0.96. That result indicates the high accuracy of Model A using three indexes based on measured luminance of Mura image to predict the ME value in the experiment.

In Model A, the indexes related to the complexity of Mura image, (g) sum of Mura edge lengths and (h) average of Mura edge circularities, were not significant. Mura images used in the experiment were produced by arranging same Gaussian shape Mura elements on 488 (28×16) places to simulate Mura of an actual LED backlight. As a result, the ranges in numerical values of these indexes were small although the statistical variabilities in these were enough. Therefore, the difference between the complexities of Mura image might be too small to affect the evaluation. In our previous study [12], the "sum of Mura edge areas," "maximum luminance difference," and "low luminance area" were important indexes for predicting the ME value. In this study, however, the "number of Mura edges" was newly shown and no "high and low luminance area," which corresponds to "low luminance area" in the previous study was shown as a significant index for predicting the ME value. We were able to point out the variations in Mura forms as a possible cause by which the "number of Mura edges" became newly significant. In the previous study, i.e., the change of index value concerning the "number of Mura edges" was not sufficiently large to predict the ME value because only five Mura form patterns were used. In the present study, however, the variations in Mura forms were sufficiently large to predict the ME value because we used more complex Mura forms than those used in the previous study. Regarding as a cause that the "high and low luminance area" was not significant, high correlation was found between indexes of the "high and low luminance area" and "maximum luminance difference" in the present study (r = 0.68–0.81, $\Delta L^* \geqq 1 - 4$). Therefore, only the "maximum luminance difference" might have become significant without the "high and low luminance area" becoming significant in Model A. It is necessary to examine whether the "high and low luminance area" is significant for predicting the ME value.

We conducted the next experiment using another set of Mura images that improves the independence between these indexes. Thereby, we confirm the accuracy of Model A.

3. Experiment 2

3.1 Methods

3.1.1 Stimuli and Apparatus

As evaluation stimulus, 46 Mura images were used. Of them, 21 Mura images were remade using the same procedure as that used in Experiment 1. The Mura pattern combinations in these 21 Mura images were selected from those in Experiment 1 according to the following procedure. Mura conditions (Table 2) were sorted in descending order of the average ME value obtained in Experiment 1, except for the flat image. Then 21 Mura conditions were selected alternately in this order from the highest rank. Bolds characters in Table 2 represent the conditions used for Experiment 2.

The other 24 Mura images were made without a high correlation between a "high and low luminance area" and a "maximum luminance difference." The "maximum luminance difference" would be almost decided by the high contrast and high arrangement density pattern, P2, P4, and P5 (Table 1, contrast range ±15, ±9, ±6%; arrangement density 90%) in the Mura image. On the other hand, the "high and low luminance area" would be decided depending on the

proportion of the low contrast patterns in the Mura image. Therefore, P2, P4, and P5 were used as the high contrast and high arrangement density pattern which would change the "maximum luminance difference." A Mura pattern with ±3% contract range and 90% arrangement density was used as the low contrast pattern, which would change the "high and low luminance area." Then, 24 Mura images were produced according to the following procedure. First, the high contrast and high arrangement density pattern of either P2, P4, or P5 was arranged in one of eight areas in the Mura image. Next, the low contrast pattern was arranged in seven remaining areas. Eight Mura images were made by changing the number of areas where the low contrast pattern was arranged from 0 to 7. Finally, the remaining areas were filled with Mura pattern with ±1% contrast range and 90% arrangement density which would not influence both indexes. We made 24 Mura images by combining the high contrast patterns of three kinds related to the "maximum luminance difference" and area numbers of the low contrast patterns of eight kinds related to the "high and low luminance area." One uniform luminance image was also tested in the experiment. The correlation coefficients between indexes of the "high and low luminance area" and the "maximum luminance difference" in these Mura images were r = 0.37–0.63 ($\Delta L^* \geqq 1-4$), and lower than r = 0.68–0.81 in Experiment 1.

The evaluation stimulus was presented with the same standard stimulus in the same experimental environment as Experiment 1. Participants evaluated 46 evaluation stimuli using the same procedure as that used in Experiment 1.

3.1.2 Participants

In this experiment, 30 participants took part (21 male and 9 female; 21–24 years of age). Each had visual acuity higher than 0.7.

3.2 Verification of Model A

In addition to Experiment 1, we standardized ME values, converted the measured luminance distribution of 46 Mura images into L^* images by the extended S-CIELAB [15], and extracted indexes related to characteristics of Mura image based on the L^* images.

Figure 5 (○) shows the relation between the ME value in Experiment 2 and the predicted ME value from Model A derived from Experiment 1. The coefficient of determination between the ME value and the predicted ME value was 0.87. The accuracy of Model A was not high to predict the ME value in Experiment 2, which indicates that Model A was derived using the indexes extracted from Mura images with high correlation between indexes so coefficients in Model A might not be appropriate to predict the ME value. In the next section, we attempt to derive the predicting model using the indexes extracted from Mura images that improves the independence between indexes in Experiment 2.

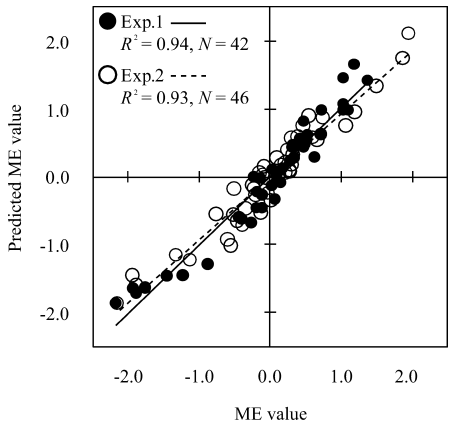

Fig. 6 Relation between the ME value and the predicted ME value calculated from Model B.

3.3 Analyses for the Predicting Model

We conducted two multiple regression analyses with data obtained from Experiment 2 and derived two models (Model B and C in Table 4). In Model B, as with Model A, (e) number of Mura edges, (f) sum of Mura edge areas, and (i) maximum luminance difference were used as explanatory variables. In model C, (a) high and low luminance area (ΔL^* = 1, which indicated the highest correlation with the ME value), in addition to three indexes in Model B, was used as explanatory variable. All explanatory variables were statistically significant. The VIFs indicate lower multicolinearity between the explanatory variables in each model. Models B and C are shown as the following equations.

$$Y = 0.0015X_e + 11.28X_f + 0.066X_i - 2.27 \quad \text{(B)}$$

$$Y = 1.58X_a + 8.77\text{E-}04X_e + 10.13X_f + 0.056X_i - 2.80 \quad \text{(C)}$$

Y: ME value, X_a–X_i: value of respective indexes

3.4 Discussion

Figure 6 shows the relation between the ME value in two experiments and the predicted ME value from Model B. The coefficients of determination between the ME value and the predicted ME value were 0.94 in Experiment 1 and 0.93 in Experiment 2. The accuracy of Model B for Experiment 2 (○) is clearly higher than that of Model A, as presented in Fig. 5. While the accuracy for Experiment 1 (●) is indicated slightly lower than that of Model A. Model B was able to predict the ME value in each experiment better than Model A did.

Figure 7 shows the relation between the ME value in two experiments and the predicted ME value from Model C. The coefficients of determination between the ME value and the predicted ME value were 0.96 in Experiment 1 and 0.94 in Experiment 2. The accuracy of Model C is higher than that of Model B. Model C was a model with an added "high and low luminance area" to Model B as an index. Therefore, this can be confirmed to show that it was useful for

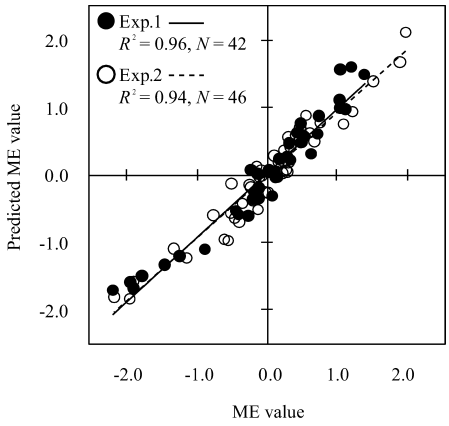

Fig. 7 Relation between the ME value and the predicted ME value calculated from Model C.

both high and low cases with the correlation between the "high and low luminance area" and the "maximum luminance difference." Moreover, many reports from the participants describe that the "high and low luminance area" was an important subjective criterion to evaluate the grade of luminance non-uniformity. Considering the two points of high accuracy and suitability as a subjective evaluation criterion, results show that Model C is the best.

4. Conclusions

In this study, we proposed a quantification method for luminance non-uniformity of a large LED backlight based on the results of two experiments. We examined the subjective evaluation for Mura of an LED backlight simulated as faithfully as possible based on a design in an actual LED backlight. So the proposed model can be applied to a quantification of subjective evaluation for Mura in an actual LED backlight that has many LED modules in array. In the proposed model, four indexes based on the measured luminance of Mura image — (a) high and low luminance area ($\Delta L^* = 1$), (e) number of Mura edges, (f) sum of Mura edge areas, and (i) maximum luminance difference — were significant as explanatory variables. This model including an index suitable for subjective evaluation criterion showed high accuracy in both experiments, suggesting that this model is effective for predicting subjectively evaluated luminance non-uniformity.

References

[1] Y. Mori, K. Tanahashi, and S. Tsuji, "Study on a method for the quantitative analysis of regions of nonuniform brightness in liquid-crystal displays," J. ITE, vol.55, no.4, pp.553–558, 2001.
[2] A. Yoshida, K. Ikuta, Y. Ohno, and M. Sato, "The luminosity spots improvement of a light emitting diode back light," IEICE Technical Report, EID2004-36, 2005.
[3] R. Yoshitake, T. Tamura, and A. Tsuji, "A proposal for a quantitative model of "Mura" level of LCDs on the basis of human senses," J. ITE, vol.56, no.7, pp.1153–1158, 2002.
[4] Y. Mori, T. Tamura, R. Yoshitake, K. Moriguchi, K. Tanahashi, and S. Tsuji, "Quantitative method of luminance non-uniformity in liquid crystal displays based on just noticeable differences," J. ITE, vol.56, no.11, pp.1837–1840, 2002.
[5] T. Tamura, M. Baba, and T. Furuhata, "Effect of the background luminance on just noticeable difference (JND) contrast of "Mura" in LCDs," Proc. IDW'03, pp.1527–1530, 2003.
[6] T. Tamura, K. Tanaka, M. Baba, M. Suzuki, and T. Furuhata, "Just noticeable difference (JND) contrast of "Mura" in LCDs on the five back-ground luminance levels," Proc. IDW'04, pp.1623–1626, 2004.
[7] T. Tamura, K. Tanaka, T. Satoh, and T. Furuhata, "Relation between just noticeable difference (JND) contrast of "Mura" in LCDs and its background luminance," Proc. IDW'05, pp.1843–1846, 2005.
[8] T. Tamura, T. Satoh, T. Uchida, and T. Furuhata, "Quantitative evaluation of luminance nonuniformity "Mura" in LCDs based on just noticeable difference (JND) contrast at various background luminances," IEICE Trans. Electron., vol.E89-C, no.10, pp.1435–1440, Oct. 2006.
[9] T. Kishi, M. Akutsu, and T. Ohtani, "Quantitative method of 'Mura' based on MTF of the human visual system," J. ITE, vol.60, no.5, pp.789–796, 2006.
[10] A.B. Watson, "The spatial standard observer: A human vision model for display inspection," SID'06 Symposium Digest of Technical Papers, vol.37, no.1, pp.1312–1315, 2006.
[11] Y. Masakura, T. Tamura, T. Satoh, and T. Uchida, "Quantitative analysis of indistinct "Mura" in displays based on subjective evaluation," J. ITE, vol.62, no.10, pp.1614–1617, 2008.
[12] Y. Masakura, T. Tamura, K. Nagamine, and S. Tomioka, "Subjective evaluation for luminance non-uniformity of LED backlight," J. ITE, vol.63, no.10, pp.1423–1428, 2009.
[13] "Recommendation 500-10; Methodology for the subjective assessment of the quality of television pictures," ITU-R Recommendations, 2000.
[14] S.S. Stevens, Psychophysics: Introduction to Its Perceptual, Neural, and Social Prospects, pp.26–31, Wiley, New York, 1975.
[15] T. Ishihara, K. Ohishi, N. Tsumura, and Y. Miyake, "Dependence of directivity in spatial frequency response of the human eye (2) — Mathematical modeling of modulation transfer function," J. Society of Photographic Science and Technology of Japan, vol.65, pp.128–133, 2002.
[16] X. Zhang and B. Wandell, "A spatial extension of CIELAB for digital color image reproduction," SID'96 Symposium Digest of Technical Papers, vol.27, pp.731–734, 1996.
[17] T. Ishihara, K. Ohishi, N. Tsumura, and Y. Miyake, "Dependence of directivity in spatial frequency response of the human eye (1) — Measurement of modulation transfer function," J. Society of Photographic Science and Technology of Japan, vol.65, pp.121–127, 2002.

Yuko Masakura received her B.E. and Ph.D. degrees from Yamaguchi University in 2000 and 2005, respectively. She was a research staff at National Institute of Advanced Industrial Science and Technology from 2005 to 2006. She has been a research staff at Tokyo Polytechnic University since 2006. She is currently engaged in research and development of evaluation method for display based on human vision and Kansei.

Tohru Tamura received his B.Sc. and Dr.Eng. degrees from the Tokyo Institute of Technology in 1985 and 1990, respectively. In 1990, he joined IBM Japan Ltd., where he was engaged in research and development of liquid-crystal displays. Since 1998 he has been with Department of Image Information Engineering, Tokyo Polytechnic University. He is now a Professor. His research fields of interests are human vision, Kansei engineering, image processing and display system.

Kunihiko Nagamine received his B.E. degree in mechanical engineering in 1993 from the Chiba University, Japan. He has been with Sony Co., since 1993, where he has engaged in the development of display devices. He is currently working in the area of the development of evaluation system for displays.

Satoshi Tomioka received the B.E. degree in applied physics in 1991 and M.E. degree in Crystalline Materials Science in 1993 from Nagoya University, Japan. Since 1993, he has been with Sony Co. During 1993–1999, he worked on laser diode for Blu-ray system. For the past ten years, he has been a display device development engineer, and now, work on evaluation system of displays.

Mitsunori Ueda received the B.E. and M.Sc. degrees in physics from the Waseda University in 1983 and 1985 respectively. He joined Sony Co. in 1985, where he has been engaged in research and development related to optical disc systems and display systems especially optics.

Yoshihide Shimpuku is General Manager of Visual Systems Development Department Core Technology Development Group, at Sony Co. He received Ph.D. degree from Osaka University in 1993.